

# **Building Penetration Loss Measurements at 900 MHz, 11.4 GHz, and 28.8 GHz**

**K.C. Allen  
N. DeMinco  
J.R. Hoffman  
Y. Lo  
P.B. Papazian**



**U.S. DEPARTMENT OF COMMERCE  
Ronald H. Brown, Secretary**

Larry Irving, Assistant Secretary  
for Communications and Information

May 1994



**CONTENTS**

	PAGE
FIGURES .....	iv
TABLES .....	ix
ABSTRACT .....	1
1. INTRODUCTION .....	1
2. DESCRIPTION OF THE EXPERIMENT .....	2
2.1 Instrumentation And Calibration .....	2
2.2 Measurement Sites .....	5
3. MEASUREMENT PROCEDURE .....	7
3.1 Radio Building .....	7
3.2 Private Residence .....	10
3.3 Storeroom With Metal Siding .....	10
4. DATA COLLECTION AND PROCESSING .....	13
4.1 Data Collection .....	13
4.2 Data Processing .....	13
5. DISCUSSION OF RESULTS .....	14
6. CONCLUSIONS .....	33
APPENDIX A: PENETRATION LOSS PLOTS FOR ALL MEASUREMENT PATHS	
A.1 Radio Building Penetration Loss .....	A-1
A.2 Private Residence Penetration Loss .....	A-39
A.3 Storeroom Penetration Loss .....	A-43

**FIGURES**

PAGE

Figure 1. ITS millimeter-wave measurement van (receiver) ..... 3

Figure 2. Remote source cart (transmitter) ..... 3

Figure 3. Wing 4 of the Radio Building with ITS millimeter-wave measurement van ..... 6

Figure 4. West side of Wing 4 of the Radio Building ..... 6

Figure 5. Private residence ..... 8

Figure 6. Storeroom with metal siding ..... 8

Figure 7. Floor plan of Wing 4 of the Radio Building with measurement paths of the transmitters ..... 9

Figure 8. Floor plan of single level wood-frame house ..... 11

Figure 9. Floor plan of building with metal siding (storeroom) .12

Figure 10. Raw data, free-space correction factor, and penetration attenuation versus distance for a typical 900-MHz measurement in the Radio Building ..... 15

Figure 11. Raw data, free-space correction factor, and penetration attenuation versus distance for a typical 11.4-GHz measurement in the Radio Building ..... 16

Figure 12. Raw data, free-space correction factor, and penetration attenuation versus distance for a typical 28.4-GHz measurement in the Radio Building ..... 17

Figure 13. Penetration loss versus distance at three frequencies for a typical run in the Radio Building ..... 18

Figure 14. Penetration loss versus distance at three frequencies for a typical run in the storeroom building with metal siding ..... 19

Figure 15. Penetration loss versus distance at three frequencies for a typical run in the private residence ..... 20

Figure 16. Cumulative distribution for all data in the Radio Building ..... 25

**FIGURES (Cont'd)**

	PAGE
Figure 17. Cumulative distribution for all data in Radio Building with just one wall between the transmitter and receiver .....	26
Figure 18. Cumulative distribution for all data in Radio Building with two or three walls between the transmitter and receiver .....	27
Figure 19. Cumulative distribution for all data in Radio Building with three or more walls between the transmitter and receiver .....	28
Figure 20. Cumulative distribution for all data in the private residence .....	29
Figure 21. Cumulative distribution for all data in the private residence with one wall between the transmitter and receiver .....	30
Figure 22. Cumulative distribution for all data in the private residence with two walls between the transmitter and receiver .....	31
Figure 23. Cumulative distribution for all data in the storeroom building with metal siding .....	32
Figure A-1. Penetration loss for Radio Building path RB1D .....	A-1
Figure A-2. Penetration loss for Radio Building path RB1E .....	A-2
Figure A-3. Penetration loss for Radio Building path RB2B .....	A-3
Figure A-4. Penetration loss for Radio Building path RB2C .....	A-4
Figure A-5. Penetration loss for Radio Building path RB3B .....	A-5
Figure A-6. Penetration loss for Radio Building path RB3C .....	A-6
Figure A-7. Penetration loss for Radio Building path RB4C .....	A-7
Figure A-8. Penetration loss for Radio Building path RB4D .....	A-8
Figure A-9. Penetration loss for Radio Building path RB5A .....	A-9
Figure A-10. Penetration loss for Radio Building path RB5B .....	A-10
Figure A-11. Penetration loss for Radio Building path RB6A .....	A-11

**FIGURES (Cont'd)**

Figure A-12. Penetration loss for Radio Building  
path RB6B .....A-12

Figure A-13. Penetration loss for Radio Building  
path RB7A .....A-13

Figure A-14. Penetration loss for Radio Building  
path RB7B .....A-14

Figure A-15. Penetration loss for Radio Building  
path RB8A .....A-15

Figure A-16. Penetration loss for Radio Building  
path RB8B .....A-16

Figure A-17. Penetration loss for Radio Building  
path RB9A .....A-17

Figure A-18. Penetration loss for Radio Building  
path RB9B .....A-18

Figure A-19. Penetration loss for Radio Building  
path RB10A .....A-19

Figure A-20. Penetration loss for Radio Building  
path RB10B .....A-20

Figure A-21. Penetration loss for Radio Building  
path RB11A .....A-21

Figure A-22. Penetration loss for Radio Building  
path RB11B .....A-22

Figure A-23. Penetration loss for Radio Building  
path RB12A .....A-23

Figure A-24. Penetration loss for Radio Building  
path RB12B .....A-24

Figure A-25. Penetration loss for Radio Building  
path RB13A .....A-25

Figure A-26. Penetration loss for Radio Building  
path RB13B .....A-26

Figure A-27. Penetration loss for Radio Building  
path RB14A .....A-27

Figure A-28. Penetration loss for Radio Building  
path RB14B .....A-28

**FIGURES (Cont'd)**

Figure A-29. Penetration loss for Radio Building  
path RB15A ..... A-29

Figure A-30. Penetration loss for Radio Building  
path RB15B ..... A-30

Figure A-31. Penetration loss for Radio Building  
path RB16A ..... A-31

Figure A-32. Penetration loss for Radio Building  
path RB16B ..... A-32

Figure A-33. Penetration loss for Radio Building  
path RB17A ..... A-33

Figure A-34. Penetration loss for Radio Building  
path RB17B ..... A-34

Figure A-35. Penetration loss for Radio Building  
path RB18A ..... A-35

Figure A-36. Penetration loss for Radio Building  
path RB18B ..... A-36

Figure A-37. Penetration loss for Radio Building  
path RB19A ..... A-37

Figure A-38. Penetration loss for Radio Building  
path RB19B ..... A-38

Figure A-39. Penetration loss for private residence  
path HL1B ..... A-39

Figure A-40. Penetration loss for private residence  
path HL1C ..... A-40

Figure A-41. Penetration loss for private residence  
path HL2A ..... A-41

Figure A-42. Penetration loss for private residence  
path HL2B ..... A-42

Figure A-43. Penetration loss for storeroom path SRR1A ..... A-43

Figure A-44. Penetration loss for storeroom path SRR1B ..... A-44

Figure A-45. Penetration loss for storeroom path SRR2A ..... A-45

Figure A-46. Penetration loss for storeroom path SRR2B ..... A-46

**FIGURES (Cont'd)**

Figure A-47. Penetration loss for storeroom path SRR3A .....A-47  
Figure A-48. Penetration loss for storeroom path SRR3B .....A-48  
Figure A-49. Penetration loss for storeroom path SRR4A .....A-49  
Figure A-50. Penetration loss for storeroom path SRR4B .....A-50  
Figure A-51. Penetration loss for storeroom path SRR5A .....A-51  
Figure A-52. Penetration loss for storeroom path SRR5B .....A-52  
Figure A-53. Penetration loss for storeroom path SRR6A .....A-53  
Figure A-54. Penetration loss for storeroom path SRR6B .....A-54  
Figure A-55. Penetration loss for storeroom path SRR7A .....A-55  
Figure A-56. Penetration loss for storeroom path SRR7B .....A-56  
Figure A-57. Penetration loss for storeroom path SRR8A .....A-57  
Figure A-58. Penetration loss for storeroom path SRR8B .....A-58

**TABLES**

PAGE

Table 1.	Mean and Standard Deviation For Radio Building Penetration Loss Path Data.....	21
Table 2.	Mean and Standard Deviation For Private Residence Penetration Loss Path Data.....	22
Table 3.	Mean and Standard Deviation For Storeroom Penetration Loss Path Data.....	22
Table 4.	Mean and Standard Deviation for Building Penetration Loss for a Variety of Combinations of Data Paths.....	23



**BUILDING PENETRATION LOSS MEASUREMENTS  
AT 900 MHZ, 11.4 GHZ, AND 28.8 GHZ**

K. C. Allen, N. DeMinco, J. R. Hoffman, Y. Lo,  
and P. B. Papazian\*

The feasibility of using radio frequencies in the super high frequency (SHF) band (3-30 GHz) for Personal Communications Services (PCS) in buildings depends on the multipath within the structure and the amount of attenuation experienced by the electromagnetic waves passing through the structures. This study measured these effects to obtain a quantitative estimate of the attenuation magnitude. This magnitude can then be used for link margin analysis to determine if personal communications at SHF is practical.

keywords: building attenuation, measurements, PCS, penetration attenuation, personal communications

## 1. INTRODUCTION

This report describes the results of a measurement program. The objective was to determine if frequencies in the super high frequency (SHF) band (3-30 GHz) can be used for Personal Communications Services (PCS) between the outside and inside of buildings in a manner like that currently used for cellular telephone at 900 MHz. The crowding of the radio frequency spectrum at 900 MHz makes it probable that PCS will be required to operate at the higher frequency bands. PCS is a class of telecommunications services that includes a wide range of capabilities, such as telephony, data transfer, paging, voice mail, and electronic messaging. PCS will provide portability and personalized telephone service to users. Many small cells similar to the cells used in cellular phone systems can be used to provide low-cost communication services through pocket-size, low-power, portable telephones to individuals wherever they may be in the service area.

The Institute for Telecommunication Sciences (ITS) has been active in the development of computer models and measurements to assess system losses in typical PCS operational environments for the proposed frequency bands. Models are being developed for urban outdoor microcells and within-building environments. The building penetration measurements described in this report will provide some insight into the degree of attenuation experienced by PCS signals when penetrating three typical structures.

---

\*The authors are with the Institute for Telecommunication Sciences, National Telecommunications and Information Administration, U.S. Department of Commerce, Boulder, Colorado 80303-3328

The experimental results in this report have been obtained to help determine the excess path loss associated with reception inside buildings and its dependence on location within the building and the building type. The data contained herein will also help to quantify the spatial variation of signal due to severe multipath.

The constructive and destructive interference at SHF frequencies are expected to vary over a much smaller spatial separation than would occur at lower frequencies and hence provide a means of obtaining space diversity reception over a short distance comparable to the size of the personal communicator set. Over a narrow bandwidth, this should minimize signal fading variations due to multipath and provide good communication performance for such a system.

This report describes the results of signal strength measurements made inside three types of buildings at three separate frequencies. The three frequencies used in the measurement were: 900 MHz, 11.4 GHz, and 28.8 GHz. The three types of buildings used for the experiment were: the ITS Wing 4 of the Department of Commerce Radio Building in Boulder, CO, (concrete construction with steel reinforcement), a private residence (wood-frame house with brick veneer), and the storeroom between Wings 3 and 5 of the Radio Building (a building with metal siding).

## **2. DESCRIPTION OF THE EXPERIMENT**

This section describes the instrumentation, calibration, and measurement sites used for the penetration measurements.

### **2.1 Instrumentation And Calibration**

The measurement system included three transmitters mounted on a cart that could be moved inside buildings, and the ITS millimeter-wave van located outside the building for reception of the signals. The van is shown in Figure 1 and the transmitter cart is shown in Figure 2. The transmitter cart consisted of three separate calibrated signal generators connected to three separate antennas. The antennas on the cart were omnidirectional in the azimuthal plane to simulate the radiation coverage typical of the small antenna that would be used for a PCS handheld unit. The receiving antennas on the van consisted of two medium-gain horn antennas with 17 dBi at 11.4 GHz and 16 dBi at 28.8 GHz both with vertical polarization, and a vertically-polarized omnidirectional antenna at 900 MHz. The beamwidths in azimuth and elevation of the 11.4-GHz horn were both 22 degrees, and the beamwidths for the 28.8-GHz horn were both 25 degrees. The horn antennas provided adequate angular coverage for receiving most of the multipath signals radiated from the transmitters inside the buildings under test, but favored the direct path and multipath signals arriving within their beamwidths.



Figure 1. ITS millimeter-wave measurement van (receiver).

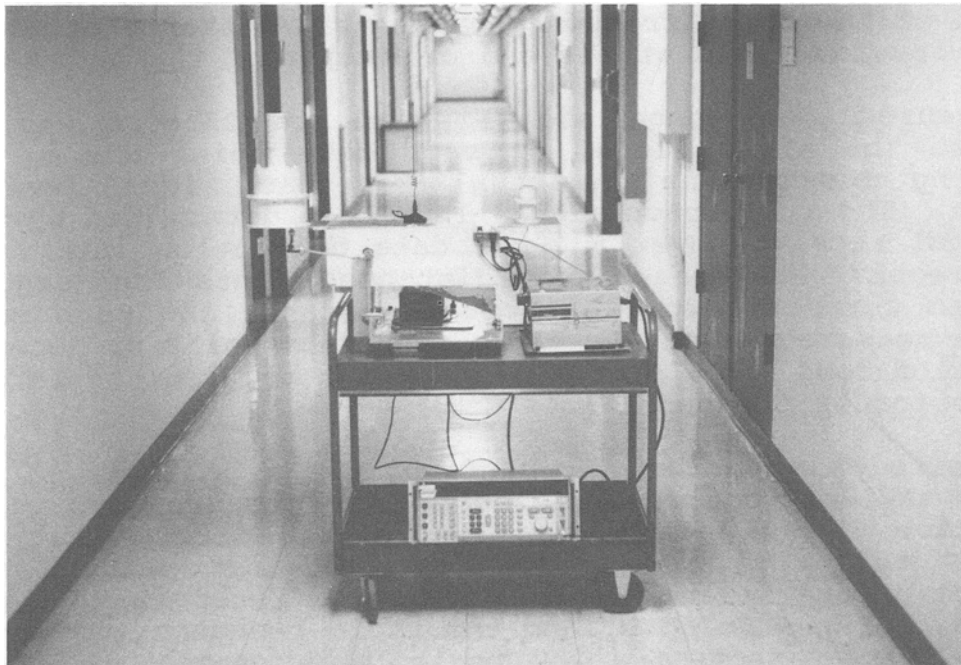


Figure 2. Remote source cart (transmitter).

This was not the case for the omnidirectional antennas. The omnidirectional antenna used at 900 MHz provided near equal response to the direct signal and all multipath signals arriving at the receiver, and therefore the destructive interference phenomenon was more likely to produce signal cancellation with deeper nulls than that attained at the higher frequencies with the horn antennas. The omnidirectional antenna vectorially adds all of the multipath return signals from all directions.

The outputs from the receiver antennas at 11.4 and 28.8 GHz were first converted down in frequency and then passed through separate logarithmic amplifiers. The output of each of the logarithmic amplifiers was a DC voltage proportional to the logarithm of the RF input power. This DC voltage was then sampled using an analog-to-digital (A/D) converter and the samples were stored in data files by a data acquisition program on the computer. The noise figure of the receiver system for the 11.4- and 28.8-GHz measurement was approximately 7 dB.

The output signal from the 900-MHz receiver antenna was applied directly to the spectrum analyzer input. The amplitude of the signal at 900-MHz was measured by the spectrum analyzer and sent to the data logging computer via the IEEE 488 BUS. The spectrum analyzer had a noise figure of approximately 20 dB at 900 MHz.

The system was calibrated to power levels relative to free space for each of the three frequency bands at a distance of 25.6 m over a grass-covered field at the end of Wing 4 of the Radio Building.

The measured free-space signal level at 25.6 m was used to normalize the signal level at each data point during the data processing to determine the actual free-space signal level at each distance. The free-space signal level was determined by averaging the signal received over a 2-min data collection interval at the 25.6-m receiver-to-transmitter distance. This free-space signal level was corrected for the actual distance and then subtracted from the measured signal level at each data point to determine the penetration loss for a signal propagating between the interior and the exterior of the building.

The received signal for all configurations consists of a direct wave and at least one wave reflected from the ground or some other obstruction. The vector addition of the direct and single or multiple reflected waves results in both constructive and destructive interference as a function of receiver-to-transmitter distance, antenna heights, and the radio frequency. The geometry for all sets of data provided a measurement of the excess attenuation experienced by the electromagnetic waves passing through the building structures for any situation that would be encountered for personal communications.

The signals at all three frequencies were sampled at sufficient intervals (1 sample/s) to characterize the data even though they were not sampled every half wavelength at the two upper frequencies (11.4 and 28.8 GHz). The linear distance between nulls and peaks for the sampled waveform created by constructive and destructive interference does not repeat every half wavelength. It is a function of the signal frequency, distance between the transmitter and receiver, transmitter antenna height, and receiver antenna height. If the receiver or transmitter moves horizontally, as was the case in the measurements performed here, the distance between two consecutive minima or maxima is given by

$$D = LR^2/2H_1H_2,$$

where D is the distance between two successive minima or maxima in meters, L is the wavelength in meters, R is the distance between the receiver and the transmitter in meters,  $H_1$  is the transmitter antenna height in meters, and  $H_2$  is the receiver antenna height in meters.

This distance was calculated for each of the three frequencies using the parameters that would result in the smallest distance between minima or maxima. The shortest distance R used during the measurements was 15 m. The transmitter height  $H_1$  was 1 m. The receiver height  $H_2$  was 3 m. The resulting distances D between minima or maxima for 900 MHz, 11.4 GHz, and 28.8 GHz were 12.50, 0.99, and 0.40 m, respectively. Referring to any of the Figures in the Appendix (A-1 through A-58), the data were sampled at least every 0.2 m, so there are at least two samples for each periodic variation of the signal as the transmitter cart was moved along all of the measurement paths. The formula above is for the periodicity of the minima and maxima variation for only the direct and reflected waves. Waves from higher order multipath signals would tend to fill in these nulls, so the case considered here is the worst-case multipath condition. The sampling of the data is therefore adequate to describe the signal fluctuation and hence compute the building attenuation.

## **2.2 Measurement Sites**

### Radio Building:

The Department of Commerce Radio Building in Boulder, CO is a concrete structure with steel reinforcement throughout. Wing 4 of the Radio Building is shown in Figure 3, with the ITS measurement van located at the end for the first sequence of measurements. There is a large amount of metal within the building for electrical conduit and structural support. The external walls of the building are concrete with re-bar reinforcement. The interior walls are mostly of cinder block with additional partitions with wood studs and gypsum dry wall. The metal-frame windows in each of the



Figure 3. Wing 4 of the Radio Building with ITS millimeter-wave measurement van.

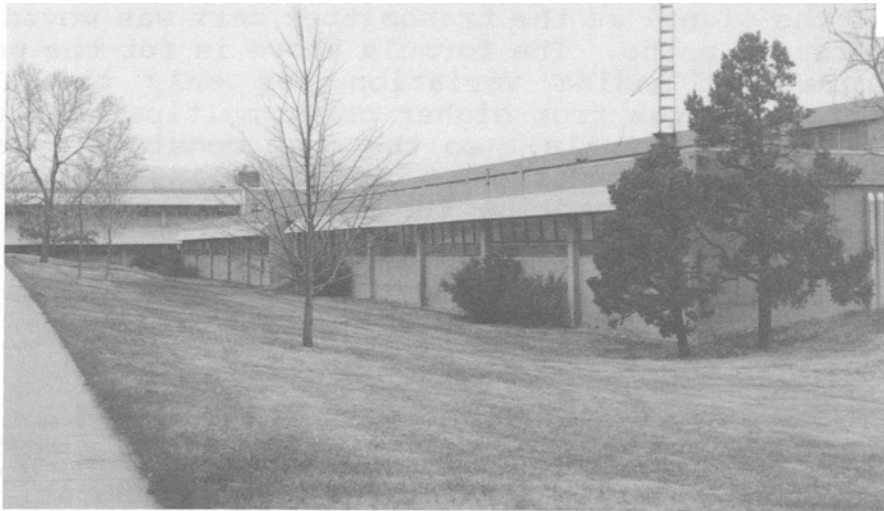


Figure 4. West side of Wing 4 of the Radio Building.

offices cover approximately 6 m<sup>2</sup>. Figure 4 is a view of the west side of Wing 4 showing these windows. All offices in Wing 4 have these windows, and as a result the building may be relatively transparent to the electromagnetic energy from the signal sources when the van was positioned on the side of the building. The office doors are of wood construction with approximately 2.3 m<sup>2</sup> of area. The rooms are filled with conventional metal office furniture including desks, file cabinets, tables, and chairs.

#### Private Residence:

The building shown in Figure 5 is a standard wood-frame house with brick veneer on the outside. The gypsum wallboard did not have a metallic foil on one side. The insulation has a paper vapor barrier. The furniture inside this structure is predominantly of wood and non-metallic construction typical of a private residence. The shrubbery and trees outside did not obstruct the line-of-sight between the transmitter and receiver. Window area on the street side of the house was approximately 4 m<sup>2</sup> per room. There were two major paths traversed during the measurement. One interior wall separated the two paths. The rear path had the exterior wall plus an interior wall between the receiver and transmitter. The front path had just one exterior wall between the receiver and the transmitter.

#### Storeroom Building With Metal Siding:

The building shown in Figure 6 is a metal frame structure with metal siding. There are a few windows, with approximately 1 m<sup>2</sup> of area each. The storeroom loading dock door and all entrance doors are made of steel. The storeroom has metal shelves along the width of the building with wide aisles between them. This structure is expected to present a large attenuation to the electromagnetic waves passing through it.

### **3. MEASUREMENT PROCEDURE**

This section describes the measurement procedure used for each of the three sites.

#### **3.1 Radio Building**

For the first set of Radio Building measurements, the signal was radiated from the cart antennas inside the building and received by the van antennas located 17.1 m from the loading dock end of Wing 4, in the driveway. Figure 7 contains a floor plan of Wing 4 of the Radio Building with the paths traversed during the measurements indicated by arrows.



Figure 5. Private residence.



Figure 6. Storeroom with metal siding.



The points of the arrows indicate the endpoints of each of the paths traversed during the measurements and the arrows indicate the direction of the path. The cart was moved down the main hallway and into offices and labs on both sides of the hallway along paths with measured distances. The receiving van was stationary during all of these measurements.

For the second set of Radio Building measurements, the signal was radiated from the cart antennas inside the building and received at the van antennas located outside the West side of the building on the sidewalk between Wing 4 and Wing 6 of the Radio Building. Figure 7 also contains the measurement paths for the new position of the van at the West side of the Radio Building. The van and the cart were located opposite each other along the length of the building wing. For a portion of the measurements, the cart was moved into some of the offices and labs on both sides of the hallway. The position of the van along the length of either wing was such that it was directly opposite of the cart. This alignment was easily performed by viewing the van through the windows of the closest office.

### **3.2 Private Residence**

For this building, the van was located in the street approximately 19.5 m from the closest outside wall. The cart was moved through several rooms along a straight line parallel to the street and data were recorded with the van stationary. The distance to the cart from the van was also determined for each data measurement group. The floor plan of the house was convenient for making two such runs and covering most of the length of the house. Figure 8 contains the floor plan with paths traversed during the measurements indicated by arrows. The arrows indicate the direction of the paths traversed during the measurements. The first path passed through the kitchen area and family room in the rear half of the house. The second path passed through the front half of the house through the dining room and living room.

### **3.3 Storeroom With Metal Siding**

For this building structure, the van was located in the parking lot of the Department of Commerce Radio Building between Wings 3 and 5, adjacent to the storeroom and approximately 17.1 m from the door. Figure 9 contains the floor plan of the storeroom with the measurement paths indicated by arrows. The points of the arrows indicate the endpoints of the paths traversed. The source cart was moved up and down all of the aisles inside the storeroom to provide a matrix of data with the variation of electromagnetic energy at three frequencies in two coordinates.

# WOOD FRAME HOUSE WITH BRICK VENEER

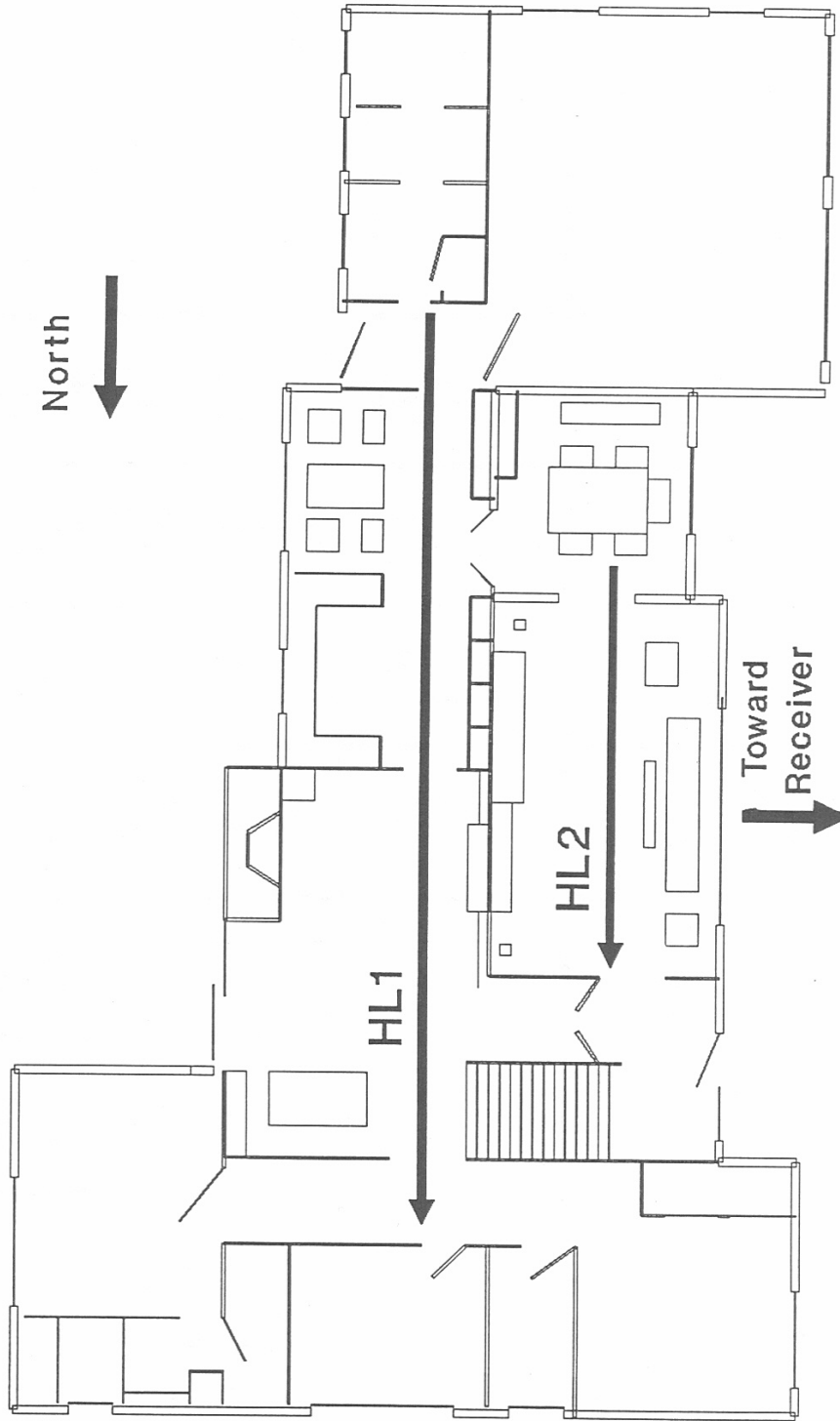


Figure 8. Floor plan of single level wood-frame house.

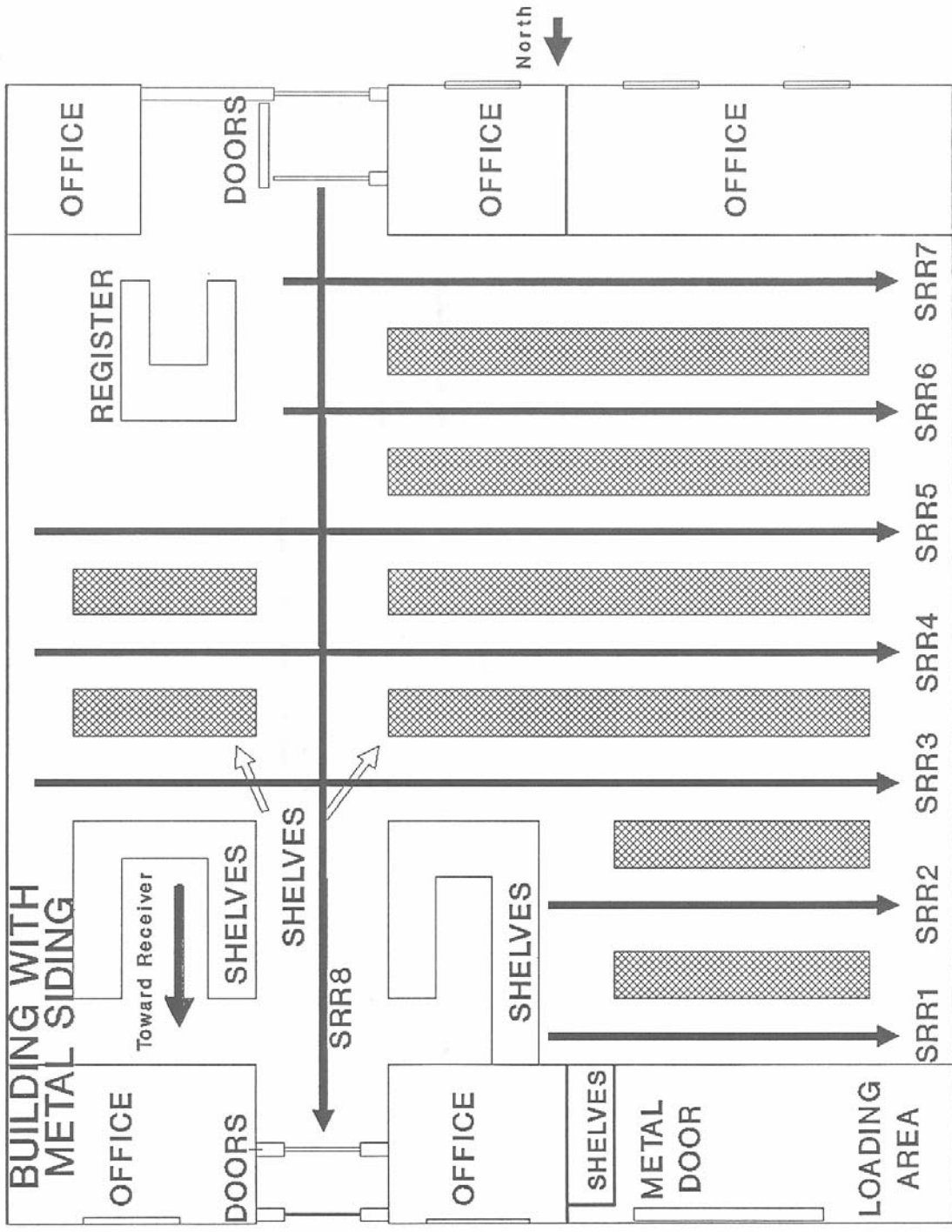


Figure 9. Floor plan of storeroom with metal siding.